



WEDNESDAY SLIDE CONFERENCE 2021-2022

Conference 19

16 February 2022

CASE I: P20-1942 (JPC 4166940)

Signalment:

A four-year-old neutered male domestic cat (*Felis catus*)

History:

Hypoxemia and respiratory distress of approximately 5 days. A presumptive diagnosis of cardiac failure in emergency room. Bloodwork revealed azotemia and hyperglycemia although glucose dropped to normal over next 24h. After 4 days of supportive care, the owner selected euthanasia. This cat was perfectly healthy previous to this episode.

Gross Pathology:

The ocular and gingival mucosa were slightly pale. Abundant (15 mL) red tinged fluid were collected from the thorax. The lungs were diffusely mottled red and slightly firm. The heart weight was 22 g. The left ventricular wall was markedly thickened, with a very narrow ventricular cavity (interpreted as hypertrophic cardiomyopathy). No significant findings in the rest of abdominal organs.

Laboratory Results:

Aerobic culture of the lung: No bacteria isolated after 48 hours. Feline Coronavirus

PCR was performed with formalin fixed paraffin embedded tissues, which was negative.

Swabs in PBS (nasal, tracheal, oropharyngeal and rectal swabs) and tissues (lung, heart) were submitted to the Animal Health Diagnostic Center at Cornell University and initially subjected to PCR testing or culture for common feline respiratory pathogens (*Bordetella sp.*, *Chlamydia felis*, *Mycoplasma cynos*, *Mycoplasma felis*, *Streptococcus equi. ssp. zooepidemicus*, influenza virus, pneumovirus, feline calicivirus and feline herpesvirus). The nasal swab sample tested positive for *M. felis* (Ct = 32), while no other common feline pathogen was detected nor isolated.

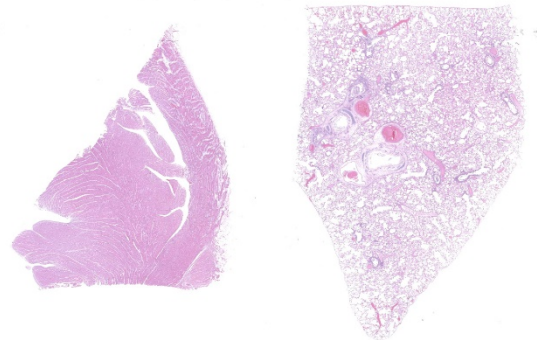


Figure 1-1. Heart, lung, cat: At subgross magnification, there is diffuse expansion of alveolar septa; there are no visible lesions at subgross magnification in the heart.

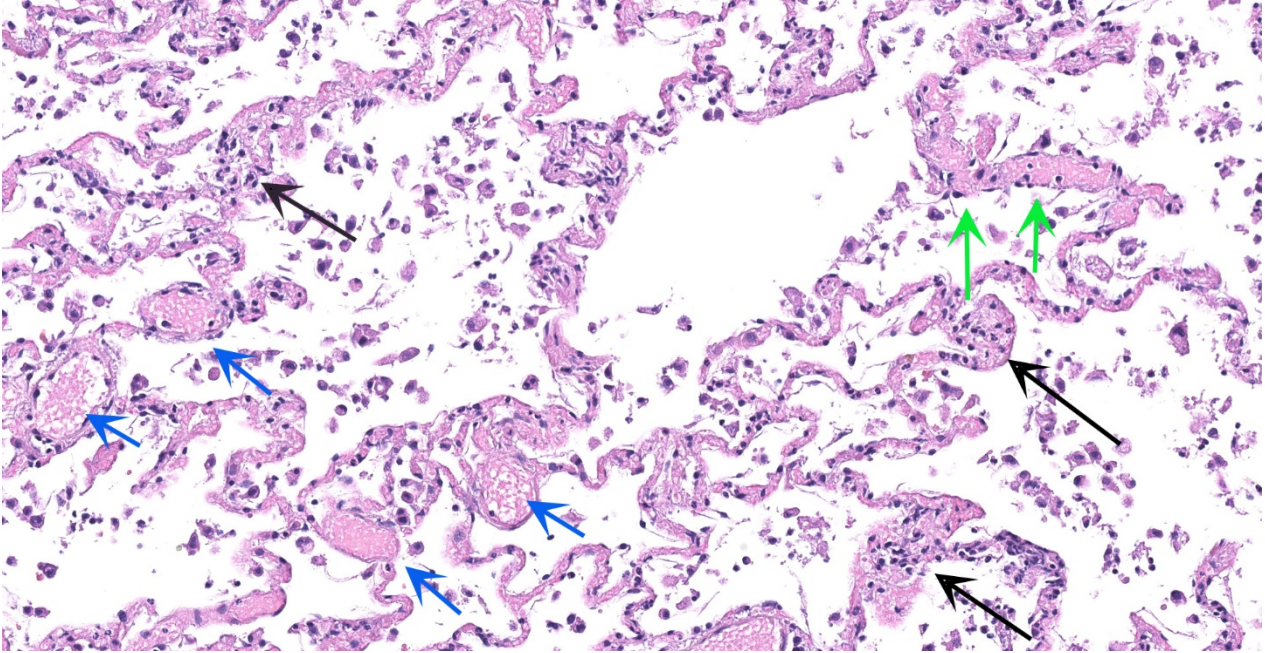


Figure 1-2. Lung, cat. There are diffuse and severe septal changes including areas of septal necrosis (black arrows), thrombosis of septal capillaries (green arrow), and thrombosis of pulmonary venules (blue arrows). (HE, 208X)

The nasal, oropharyngeal, tracheal and rectal swabs were positive for SARS-CoV-2 when tested by real-time RT-PCR assay (rRT-PCR). This result was later confirmed by NVSL. Immunohistochemistry and *in situ* hybridization for SARS-CoV-2 staining revealed strong viral labeling/staining in bronchial epithelial cells, bronchiolar glands, bronchiolar epithelium and in few desquamated epithelial cells/macrophages in alveolar spaces.

Microscopic Description:

Lung: An acute bronchointerstitial pneumonia was noted. In bronchi, there was circumferential degeneration and necrosis of bronchial epithelial cells, with focal infiltrates of viable and degenerate neutrophils and macrophages. Similar inflammatory infiltrates were present surrounding bronchial glands. Necrosis of epithelial cells and similar inflammation was identified in the bronchiolar lumen, with some being completely occluded with cellular debris. In alveoli, damage was characterized by numerous macrophages

with frequent phagocytosis of cellular debris, presence of multinucleated cells suggesting syncytial cells and a few neutrophils, all immersed in edema, multifocal hemorrhages, and fibrin, with the formation of rare hyaline membranes. There was multifocal mild segmental hyperplasia of type II pneumocytes. The alveolar septa were thickened with increased numbers of intravascular neutrophils and multiple segments of necrotizing capillaritis, with microthrombi and focal dense infiltrates of neutrophils and macrophages. Occasional arteries have transmural infiltrates of mononuclear cells with margination of neutrophils.

Heart: There was multifocal to coalescing areas of degeneration and necrosis of cardiomyocytes, with cells displaying hypereosinophilic cytoplasm, loss of striations, hypercontraction bands, vacuolation and or pyknotic nuclear debris. There was edema with the presence of small numbers of macrophages and neutrophils between myofibers. In addition, there was

mild concentric hypertrophy of the left ventricle. Cardiomyocytes have moderate variation of the cytoplasmic diameter, feature that was more frequent towards the periphery of the myocardium.

Contributor’s Morphologic Diagnoses:

1. Lung: Pneumonia, bronchointerstitial, neutrophilic and histiocytic, acute to subacute, severe, with bronchial/bronchiolar necrosis, vascular thrombi and multifocal capillaritis.
2. Heart: Myocardial degeneration and necrosis, severe, multifocal to coalescing, with mild neutrophilic and histiocytic myocarditis.

Contributor’s Comment:

Human to animal transmission and natural infections with SARS-CoV-2 have been reported in domestic cats, dogs, and ferrets as well as in wild animals in zoological collections around the world including tigers, lions and puma.^{13,14,16,20,23,24,25} Most SARS-CoV-2 infections in animals have been

associated with subclinical- or only with mild clinical signs in affected animals.^{8,22,26}

The predominant histologic pulmonary lesion in human patients that develop pneumonia due to the infection with SARS-CoV-2 is diffuse alveolar damage (DAD), including the exudative, proliferative and fibrotic phases or a mixture of these, with various levels of progression and severity. Changes include edema, congestion and formation of hyaline membranes, hyperplasia of atypical type II pneumocytes (reactive atypia) and increased numbers of macrophages and lesser neutrophils in the alveolar lumen; interstitial thickening with vascular thrombosis, CD4+ and CD8+ lymphocytes and macrophages infiltrates, endothelialitis and variable interstitial proliferation of myofibroblasts.^{1,2,4,6,7,10,11,12,18,21,28} Similar to the findings in humans, the histological changes observed in the lung of the cat in this study are indicative of DAD, with segmental proliferation of atypical type II pneumocytes (reactive atypia), thrombosis and focal areas of

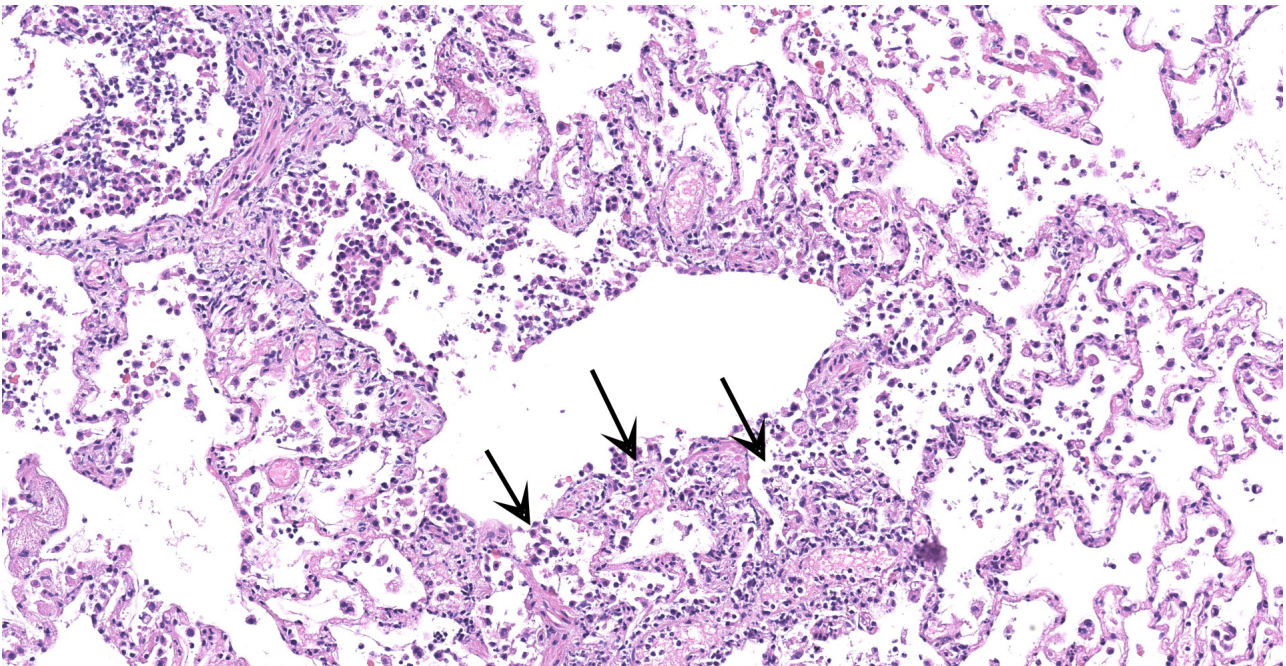


Figure 1-3. Lung, cat. In addition to changes described in fig 1-2, there is necrosis of airway epithelium, which is especially prominent at the bronchoalveolar rim (arrows). (HE, 156X)

capillaritis and the inflammatory infiltrate being mainly composed of neutrophils and macrophages, which support an early disease stage. The infection was confirmed by IHC and ISH, suggesting direct viral damage to the lung.

The reported histological findings of the human heart in cases of severe SARS-CoV-2 infection are variable and range from no lesions, to a few interstitial mononuclear inflammatory infiltrates to myocardial degeneration and necrosis without significant inflammation.^{5,12,21,28} Histological examination of the heart of the cat in this case revealed acute myocardial degeneration and necrosis, with mild interstitial acute inflammation. These observations are compatible with an early manifestation of viral myocarditis but could also be secondary to a disseminated vascular damage.

One interesting finding of this case was the fact that the animal was affected by mild hypertrophic cardiomyopathy (HCM) with no previous clinical manifestations, as evidenced at necropsy by an enlarged ventricular wall and a narrow-left ventricle. The association of underlying cardiovascular disease and myocardial injury with severe and often fatal outcomes of COVID-19 in human patients has been well documented.¹⁵ It has been suggested that patients with hypertrophic cardiomyopathy have an

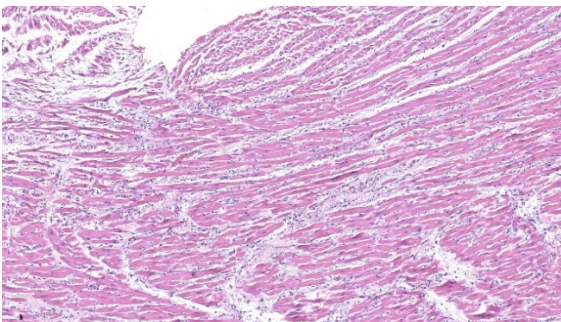


Figure 1-4. Heart, cat. There is marked edema with a mild to moderate cellular infiltrate separating myofibers, most prominently in the right ventricle. (HE, 100X)

increased ACE2 gene expression in the heart, which could be associated with an increased risk for severe COVID-19 manifestations in HCM patients.^{3,29} It is not known if cats with HCM have increased expression of the ACE2 gene. However, the fact that HCM has been observed as a comorbidity in other cats diagnosed with SARS-CoV-2 and that presented severe progressive respiratory disease,²⁴ support the hypothesis that this common heart condition in cats could indeed predispose severe disease and poor prognosis in domestic cats that become infected with SARS-CoV-2.

Contributing Institution:

Virginia Maryland College of Veterinary Medicine.

205 Duck Pond Dr

Blacksburg, VA 24061

<https://vetmed.vt.edu/departments/biomedical-sciences-and-pathobiology.html>

JPC Diagnosis:

1. Lung: Pneumonia, bronchointerstitial, necrotizing and neutrophilic, diffuse, moderate, with multifocal septal necrosis and thrombosis.

2. Heart: Myofiber degeneration, necrosis, and loss, multifocal, with mild to moderate histiocytic and neutrophilic myocarditis, and edema.

JPC Comment:

The contributor provides a concise comparison of histological features characteristic of severe acute respiratory syndrome virus (SARS-CoV-2) infection in both humans and domestic felines.

SARS-CoV-2 is the etiologic agent of Coronavirus Disease 2019 (COVID-19). First identified in Wuhan City, Hubei Province, China in December 2019, COVID-

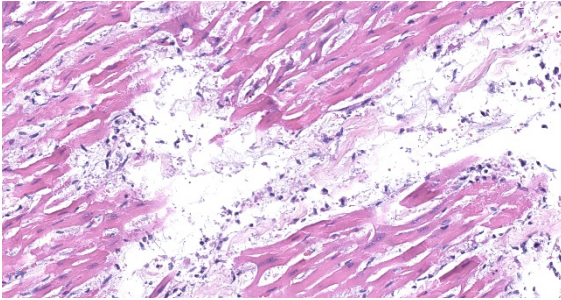


Figure 1-5. Heart, cat. In areas of edema, there is degeneration, necrosis, and loss of myofibers with interstitial infiltration of low numbers of macrophages and neutrophils. (HE, 249X)

19 quickly evolved into the ongoing and continually evolving global pandemic.¹⁷

SARS-CoV-2 is one of several species of the *Betacoronavirus* (β CoV) genus, which falls under the *Coronaviridae* and *Orthocoronavirinae* family and subfamily, respectively. In addition to β CoV, the *Orthocoronavirinae* subfamily includes genera *Alphacoronavirus* (α CoV), *Deltacoronavirus* (δ CoV), and *Gamma-coronavirus* (γ CoV). These enveloped viruses contain a single-strand, positive-sense RNA genome, are 80-220 nm in diameter, and infect a wide spectrum of wild and domestic species. In addition, a characteristic feature shared by these viruses is a unique “crown-like” appearance (*corona*: Latin for “crown”) when viewed via electron microscopy due to the presence of superficial spike proteins.¹⁷

Avian species are primarily infected by δ CoVs and γ CoVs (e.g. avian CoV – infectious bronchitis virus) with some spillover into mammals; α CoVs and β CoVs are restricted to mammals. Examples of α CoVs include feline infectious peritonitis virus and transmissible gastroenteritis virus in swine. Examples of β CoVs include bovine CoV and sialodacryoadenitis virus of rats in addition the highly pathogenic human β CoVs, which include severe acute respiratory syndrome (SARS) CoV-1,

Middle East respiratory syndrome (MERS) CoV, and SARS-CoV-2.¹⁷

Coronaviruses are prone to mutation and recombination, greatly facilitating their propensity to not only undergo cross-species transmission, but also adapt and replicate in new host species following a spillover event. Examples of spillover events in veterinary species include the emergence of bovine CoV from equine CoV in the 1700s and more recently with both porcine epidemic diarrhea virus and swine acute diarrhea syndrome virus originating from bat strains. Notably, both SARS-CoV-1 and MERS CoV also originated from bat strains and infected intermediate hosts, civit cats and dromedary camels, respectively, prior to infecting humans. SARS-CoV-2 is suspected to have also undergone a similar host switching process, although the intermediate host is uncertain. Unfortunately, future spillover events into economically important livestock species and the human population are highly likely, particularly given the history of coronaviruses exhibiting a panache for interspecies transmission.¹⁷

As noted by the contributor, human to animal (i.e. reverse zoonosis) transmission of SARS-CoV-2 has been reported in multiple species, including domestic canines and felines, mink, and large cats in zoo collections.²⁷ In addition, research models utilized include both old and new world non-human primates, mice, ferrets, cats, and hamsters. The majority of animal models utilized for research and development of SARS-CoV-2 prophylactics and therapeutics are nonhuman primates, Syrian hamsters, and mice.²⁰

Research in regard to the pathogenesis of SARS-CoV-2 is ongoing. However, a key feature of the virus is its specific targeting of the angiotensin converting enzyme-2 (ACE2) receptor on host cell membranes. Multiple

cell types express ACE2 receptors, including type I & II pneumocytes, endothelial cells, myocardiocytes, cholangiocytes, enterocytes, and oral mucosal epithelium.⁹ Once bound by the spike protein, proteases such as transmembrane serine protease 2, cathepsin B or L, or furin cleave the spike protein, leading to fusion with the host cell's membrane, infection, and ensuing cytopathic effects. Systemic disturbances may also occur, such as dysregulation of blood pressure due to downregulation of ACE2 receptors.¹⁷ Furthermore, it has been hypothesized human patients with certain underlying conditions, such as hypertension or COPD, are at increased risk due to upregulation of ACE2 receptors.²¹

In addition to respiratory disease, SARS-CoV-2 infection has also been reported to cause encephalitis, cerebral microhemorrhages, stroke, and diffuse leukoencephalopathy in humans. These lesions are hypothesized to occur due to viral binding to ACE2 rich endothelial cells in the CNS. In addition, both glial cells and neurons are reported to express ACE2 and may be targets of infection.⁹

The moderators discussed the importance of identifying and developing animal models that recapitulate lesions found in humans to allow effective and ethical investigation human diseases, such as with SARS-CoV-2. As noted by the contributor, most SARS-CoV-2 infections in humans are relatively mild, however severe disease tends to be associated with comorbidities, such as hypertension. Therefore it is important to identify animal models that not only represent the human population as a whole but also smaller subsets that may help identify "at risk" groups while also developing effective countermeasures applicable to those populations.

Conference participants also reviewed additional histochemical stains from this case, with Masson's trichrome revealing alveolar septa are mildly expanded by fibrosis. Participants hypothesized this case may have initially manifested as a subclinical chronic infection that was masked given typical feline behavior, followed by decompensation as the patient became hypoxic and ultimately presented in respiratory distress.

References:

1. Ackermann M, Verleden SE, Kuehnel M, et al. Pulmonary vascular endothelialitis, thrombosis and angiogenesis in COVID-19. *N Engl J Med*. 2020; 383: 120-128.
2. Borczuk AC, Salvatore SP, Seshan SV, et al. COVID-19 pulmonary pathology: a multi-institutional autopsy cohort from Italy and New York City. *Modern Pathol*. 2020; 33: 2156-2168.
3. Bos JM, Hebl VB, Oberg AL, et al. Marked Up-Regulation of ACE2 in Hearts of Patients With Obstructive Hypertrophic Cardiomyopathy: Implications for SARS-CoV-2-Mediated COVID-19. *Mayo Clin Proc* 2020; 95, 1354–1368
4. Bryce C, Grimes Z, Pujadas E, et al. Pathophysiology of SARS-CoV-2: targeting endothelial cells renders a complex disease with thrombotic microangiopathy and aberrant immune response. The mount Sinai COVID-19 autopsy experience. medRxiv 2020.05.18.20099960
5. Buja LM, Wolf DA, Zhao B, et al. The emerging spectrum of cardiopulmonary pathology of the coronavirus disease 2019 (COVID-19): Report of 3 autopsies from Houston, Texas, and review of autopsy findings from other United States cities. *Cardiovasc Pathol*. 2020; 48: 107233.

6. Calabrese F, Pezzutto F, Fortarezza F, et al. Pulmonary pathology and COVID-19: lessons from autopsy. The experience of European pulmonary pathologists. *Virchows Archiv* 2020; 477: 359-372.
7. Carsana L, Sonzogni A, Nasr A, et al. Pulmonary post-mortem findings in a series of COVID-19 cases from northern Italy: a two-centre descriptive study. *Lancet Infect Dis* 2020; 20: 1135-1140.
8. Chandrashekar A, Liu J, Martino AJ, et al. SARS-CoV-2 infection protects against rechallenge in rhesus macaques. *Science* 2020; 369: 812-817.
9. Choudhary S, Kanevsky I, Yildiz S, et al. Modeling SARS-CoV-2: Comparative Pathology in Rhesus Macaque and Golden Syrian Hamster Models [published online ahead of print, 2022 Feb 5]. *Toxicol Pathol.* 2022;1926233211072767.
10. Damiani S, Fiorentino M, De Palma A, et al. Pathological post-mortem findings in lungs infected with SARS-CoV-2. *J Pathol* 2021; 263: 31-40.
11. Edler C, Schröder AS, Aepfelbacher M, et al. Dying with SARS-CoV-2infection – an autopsy study of the first consecutive 80 cases in Hamburg, Germany. *Int J Legal Med* 2020, 134: 1275-1284.
12. Fox SE, Akmatbekov A, Harbert JL, et al. Pulmonary and cardiac pathology in African American patients with COVID-19: an autopsy series from New Orleans. *Lancet Res Med* 2020; 8: 681-686.
13. Gaudreault NN, Trujillo JD, Carossino M, et al. SARS-CoV-2 infection, disease and transmission in domestic cats. *Emerg Microbes Infect.* 2020; 9: 2322-2332.
14. Gortázar C, Barroso-Arévalo S, Ferreras-Colino E, et al. Natural SARS-CoV-2 infection in kept ferrets, Spain. *Emerg Infect Dis.* 2021; 27: 1994-1996.
15. Guo T, Fan Y, Chen M, et al, Cardiovascular Implications of Fatal Outcomes of Patients with Coronavirus Disease 2019 (COVID-19). *JAMA Cardiol.* 2020; 5: 811-818.
16. Halfmann PJ, Hatta M, Chiba S, et al. Transmission of SARS-CoV-2 in domestic cats. *N Engl J Med* 2020; 383; 592-594.
17. Kenney SP, Wang Q, Vlasova A, Jung K, Saif L. Naturally Occurring Animal Coronaviruses as Models for Studying Highly Pathogenic Human Coronaviral Disease. *Vet Pathol.* 2021;58(3):438-452.
18. Keresztes AA, Perde F, Ghita-Nanu A, et al. Post mortem diagnosis and autopsy findings in SARS-CoV-2 infection. Forensic case series. *Diagnostics* 2020; 10: 1070.
19. Kumar A, Prasoon P, Kumari C, et al. SARS-CoV-2-specific virulence factors in COVID-19. *J Med Virol.* 2021;93(3):1343-1350.
20. McAloose D, Laverack M, Wang L, et al. From people to panthera: Natural sars-cov-2 infection in tigers and lions at the bronx zoo. *MBio.* 2020; 11: 1–13.
21. Martines RB, Ritter JM, Matkovic E, et al. Pathology and pathogenesis of SARS-CoV-2 associated with fatal Coronavirus disease, United States. *Emerg Infect Dis* 2020; 26: 2005-2015.
22. Munster VJ, Feldmann F, Williamson BN, et al. Respiratory disease in rhesus macaques inoculated with SARS-CoV-2. *Nature.* 2020; 585: 268–272.
23. Patterson EI, Elia G, Grassi A, et al. Evidence of exposure to SARS-CoV-2 in cats and dogs from households in Italy. *Nat. Commun.* 2020; 11: 1–5.
24. Segalés J, Puig M, Rodon J, et al. Detection of SARS-CoV-2 in a cat owned by a COVID-19-affected patient in Spain. *PNAS* 2020; 117: 24790-24793.
25. Sit THC, Brackman CJ, Ip SM, et al. Infection of dogs with SARS-CoV-2. *Nature* 2020; 586: 776-778.
26. Shi J, Wen Z, Zhong G, et al. Susceptibility of ferrets, cats, dogs, and

- other domesticated animals to SARS-coronavirus 2. *Science* 2020; 36: 1016–1020
27. Sooksawasdi Na Ayudhya S, Kuiken T. Reverse Zoonosis of COVID-19: Lessons From the 2009 Influenza Pandemic. *Vet Pathol.* 2021;58(2):234-242.
 28. Xu Z, Shi L, Wang Y, et al. Pathological findings of COVID-19 associated with acute respiratory distress syndrome. *Lancet Respir Med* 2020; 8: 420-422.
 29. Zhang H, Penniger JM, Li Y, et al. Angiotensin-converting enzyme 2 (ACE2) as a SARS-CoV-2 receptor: molecular mechanisms and potential therapeutic target. *Intensive Care Med* 2020; 46: 586-590.
 30. Patania OM, Chiba S, Halfmann PJ, et al. Pulmonary lesions induced by SARS-CoV-2 infection in domestic cats [published online ahead of print, 2021 Dec 29]. *Vet Pathol.* 2021;3009858211066840.
 31. Rotstein DS, Peloquin S, Proia K, et al. Investigation of SARS-CoV-2 infection and associated lesions in exotic and companion animals [published online ahead of print, 2022 Jan 18]. *Vet Pathol.* 2022;3009858211067467.
 32. Choudhary S, Kanevsky I, Yildiz S, et al. Modeling SARS-CoV-2: Comparative Pathology in Rhesus Macaque and Golden Syrian Hamster Models [published online ahead of print, 2022 Feb 5].

CASE II: 19-31-3 (JPC 4166464)

Signalment:

Adult Syrian hamster (*Mesocricetus auratus*)

History:

An adult Syrian hamster was evaluated by veterinary staff at the University of North Carolina - Chapel Hill for signs of malaise, including a hunched posture, dehydration,

weight loss, and facial swelling with patchy alopecia. Eight weeks earlier, the hamster had arrived from an academic institution with 19 other male and female hamsters. The hamsters were STAT2 knockouts that were purchased for a respiratory syncytial virus study and were clinically healthy upon arrival. The hamsters had not yet been infected with respiratory syncytial virus. Upon physical examination, the hamster had multiple cutaneous masses along the face and limbs. Many of the other hamsters had similar cutaneous masses and/or a firm palpable abdominal mass. The entire cohort was culled.

Gross Pathology:

Bilaterally along the haired skin overlying the cheek pouches, ventral mandible, and limbs, there were innumerable, multifocal to coalescing, 2-20 mm in diameter, raised, semi-firm, pale pink to grey, cutaneous masses with varying degrees of alopecia. A draining tract associated with the masses along the left cheek pouch was present. Bilaterally along the mucosa of the cheek pouches, there were innumerable, multifocal,



Figure 2-1. Presentation, hamster: Bilaterally along the haired skin overlying the cheek pouches, ventral mandible, and limbs, there were innumerable, multifocal to coalescing, 2-20 mm in diameter, raised, semi-firm, pale pink to grey, cutaneous masses. (Photo courtesy of: University of North Carolina - Chapel Hill - <https://research.unc.edu/comparative-medicine/>)



Figure 2-2. Oral cavity: Bilaterally along the mucosa of the cheek pouches, there were innumerable, multifocal, pinpoint to 3 mm in diameter, exophytic, pale tan, firm, papillomatous masses (Photo courtesy of: University of North Carolina - Chapel Hill <https://research.unc.edu/comparative-medicine/>).

pinpoint to 3 mm in diameter, exophytic, pale tan, firm, papillomatous masses.

Laboratory Results:

Prior to arrival, this hamster tested serologically positive for hamster polyomavirus and negative for *Encephalitozoon cuniculi*, lymphocytic choriomeningitis virus, pneumonia virus of mice, reovirus 3, Sendai virus, simian virus 5, *Clostridium piliforme*, and were PCR negative for pinworms and fur mites. PCR for papillomavirus on samples of the cheek pouch tumors was negative. Electron microscopy on the skin tumors did not reveal any viral particles.

Microscopic Description:

Haired skin, oral mucosa (cheek pouch): Three sections of cheek pouch containing haired skin and oral mucosa are examined. Markedly expanding the dermis are multifocal to coalescing, unencapsulated, well demarcated, neoplastic masses with a cystically dilated central cavity and a superficial pore that communicates with the surface. Cystic centers resemble dilated

infundibula and have a wall of stratified squamous epithelium with keratohyalin granules and orthokeratotic stratum corneum which accumulates centrally. Connected to and radiating from the cystic cavities are multiple linear primitive hair follicle structures with distinct follicular differentiation (structure and cytodifferentiation): matrical cell differentiation (forming hair bulbs), internal root sheaths with red trichohyalin granules, vacuolated external root sheaths (agranular), and occasional abortive hair shafts with ghost cell cornification. Connected to the linear follicle structures are multifocal, small lobules of epithelial cells resembling well-differentiated sebocytes. There are 82 mitotic figures per 10 high power fields (area 2.37 mm²) with occasional bizarre mitoses; the mitotic rate is most prominent within matrical cell differentiated populations. There is mild anisocytosis and anisokaryosis. There is frequent necrosis of individual neoplastic cells throughout all components. Areas of central cornification within cystic infundibular structures occasionally contain

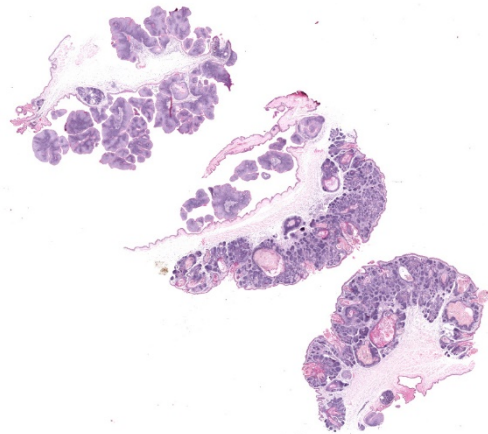


Figure 2-3. Haired skin and oral mucosa, hamster. Three sections are submitted for examination. At top left is oral mucosa with multiple papillomas. The middle section is a full-thickness section of cheek with cheek pouch, papillomas on the mucosal side. The section at lower right is a section of haired skin with a follicular neoplasm as well. (HE, 481X)

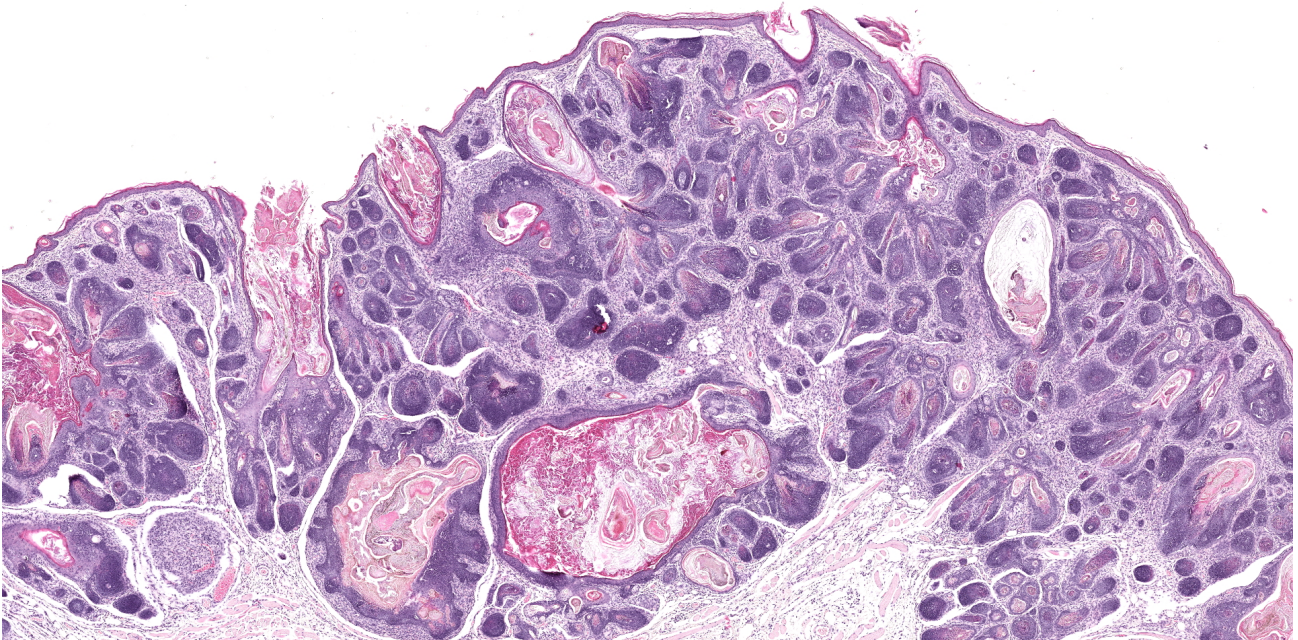


Figure 2-4. Haired skin, cheek, hamster. Expanding the dermis, there is a well-demarcated neoplasm composed of abortive attempts of folliculogenesis opening into central cystic cavities, which occasionally extend to the overlying epidermis. (HE, 27X)

small colonies of coccoid bacteria with few viable and degenerative heterophils. The masses are separated by a fibrovascular stroma composed of moderately increased numbers of plump fibroblasts within a loose collagenous matrix containing numerous small caliber blood vessels. Scattered throughout the supporting stroma are moderately increased numbers of perivascular to interstitial mast cells and few heterophils.

The mucosal epithelium is multifocally, markedly expanded by unencapsulated, well-demarcated, exophytic papillary masses composed of well-differentiated squamous epithelium that is supported by a thin fibrovascular stalk. The neoplastic epithelial cells are polygonal and have distinct cell borders, a moderate amount of eosinophilic cytoplasm, and a central round nucleus with 0-1 prominent nucleoli, and finely stippled chromatin. There is moderate anisocytosis and anisokaryosis.

There are 66 mitotic figures per 10 high power fields (area 2.37 mm²). There is frequent necrosis of individual neoplastic cells. Occasionally, the masses along the oral mucosa contain central sebocyte differentiation and basilar trichoblastic differentiation as described within the masses in the haired skin (above). The supporting stroma is multifocally infiltrated by moderate numbers of mast cells, fewer heterophils, and rare lymphocytes and plasma cells. Along the overlying stratum corneum, there are occasional, small colonies of coccoid bacteria.

Contributor's Morphologic Diagnoses:

Cheek pouch:

1. Haired skin: Multifocal to coalescing trichoepitheliomas with bacterial colonization and mild heterophilic dermatitis.
2. Buccal mucosa: Multifocal squamous papillomas with minimal adnexal differentiation and mild heterophilic stomatitis.

Contributor's Comment:

The gross and histopathologic haired skin lesions in this case are consistent with trichoepitheliomas secondary to hamster polyomavirus (HaPyV) infection in a signal transducer and activator of transcription protein 2 (STAT2) knockout hamster.

HaPyV is a non-enveloped, double stranded DNA virus that is reported to cause trichoepitheliomas and epizootic transmissible lymphoma in hamsters.²⁻⁷ Other tumor types associated with HaPyV have not been described.¹ Prevalence of HaPyV is uncommon in laboratory hamster populations.¹ In this case, immunosuppression likely predisposed this hamster to infection and tumorigenesis by HaPyV. Animals without STAT2 are unable to transcriptionally respond to interferons resulting in increased susceptibility to viral infections.^{5,9} Lymphoma typically occurs within epizootically infected populations, whereas enzootically infected populations are more prone to developing trichoepitheliomas.^{2,3} Trichoepitheliomas develop in hamsters 3-12 months of age. Lymphoma in HaPyV infected hamsters typically develops in young hamsters.²⁻⁶

Transmission of HaPyV is thought to occur by ingestion of infected feces or urine (hamsters are naturally coprophagic).^{2,6} HaPyV persists within renal tubular epithelium and is shed into the urine and can also be present in infected keratinocytes and enterocytes within feces.² HaPyV has a tropism for undifferentiated keratinocytes and lymphocytes, resulting in trichoepitheliomas and lymphoma, respectively. Trichoepitheliomas typically arise on the face and feet, although they can be found anywhere on the body. Lymphoma most often develops within the mesentery, intestines, liver, kidney, and thymus.^{2,3,6} HaPyV may replicate within cells resulting in lysis or transform cells without replication.

Similar to papillomaviruses, HaPyV exhibits viral replication within trichoepitheliomas.

While HaPyV is oncogenic, tumor development is not critical to viral survival and replication. Therefore, hamsters can be subclinically infected.²

Diagnosis of HaPyV associated disease is typically made on histologic diagnosis of trichoepitheliomas and lymphoma. Trichoepitheliomas unassociated with HaPyV have not been described, and lymphoid tumors unassociated with HaPyV are uncommon in young hamsters. Further diagnostics may include virus isolation, PCR, serology, and electron microscopy. Prior to arrival at UNC - Chapel Hill, the hamster tested serologically positive for HaPyV. The negative electron microscopy results in this case do not rule out HaPyV as finding virions on electron microscopy is often challenging.²

To our knowledge, oral papillomas or other oral tumors have not been reported with HaPyV infected hamsters. Given the mild adnexal differentiation associated with the papillomas along the oral mucosa in this case, these tumors are thought to have arisen from HaPyV infection. A lack of further

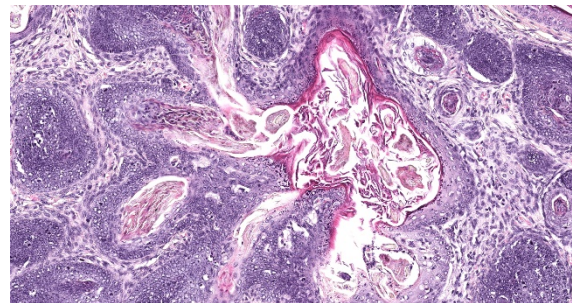


Figure 2-5. Haired skin, cheek, hamster. The neoplasm is composed of multiple lobules composed of attempts of follicle formation with cells resembling the outer root sheath, which develop a glassy, clear cytoplasm before undergoing abrupt keratinization without the interposition of a granular layer (tricholemmal keratinization). (HE, 191X)

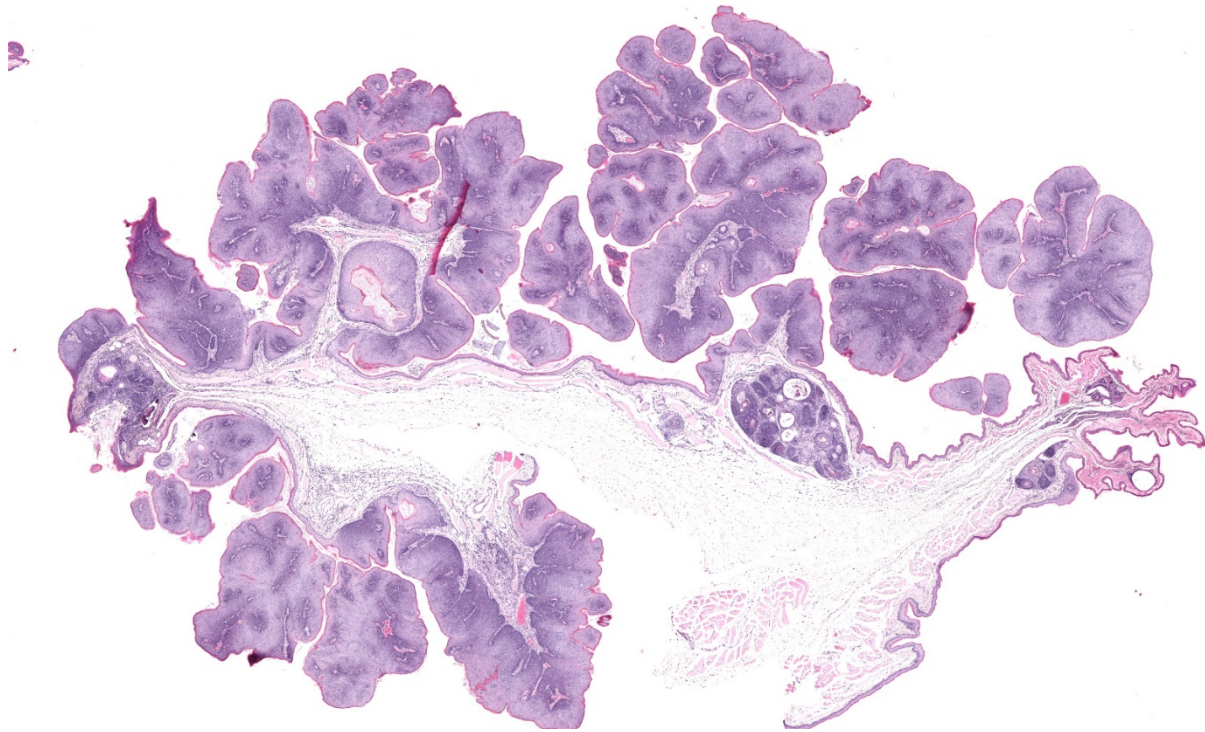


Figure 2-6. Oral mucosa, cheek, hamster. The oral mucosa is covered with numerous squamous papillomas. (HE, 13X)

trichoepithelial differentiation within this population of tumors may be due to the absence of follicular epithelium along the oral mucosa. Samples of the cheek pouch tumors tested negative for papillomavirus on PCR.

In conclusion, this report describes a case of trichoepitheliomas and oral squamous papillomas, thought to be caused by HaPyV.

Contributing Institution:

1. University of North Carolina - Chapel Hill
 - a. <https://research.unc.edu/comparative-medicine/>
2. North Carolina State University
 - a. <https://cvm.ncsu.edu/research/departments/dphp/>

JPC Diagnosis:

1. Haired skin: Trichofolliculomas, multiple.

2. Oral mucosa: Squamous papillomas, multiple.

JPC Comment:

The contributor provides a concise review of the epizootology, associated lesions, and diagnosis of hamster polyoma virus (HaPyV), one of the first rodent polyomaviruses identified. HaPyV was discovered in the late 1960s in a colony of Syrian hamsters (*Mesocricetus auratus*) affected by skin tumors. Ensuing research in Germany found viral particles extracted from the skin tumors caused lymphoma and leukemia when injected into neonatal hamsters.³ Research published by Barthold et al. in 1987 further evaluated its transmission, reporting the development of lymphoma in previously unexposed weanling hamsters that were subsequently maintained in both direct and indirect contact with hamsters previously exposed to HaPyV,

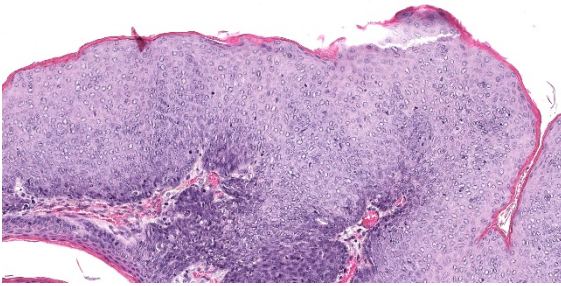


Figure 2-7. Oral mucosa, cheek, hamster. The mucosal epithelium is thickened up to 5X normal with a markedly expanded stratum spongiosum. (HE, 201X)

which was known as hamster papovavirus at the time.¹

A key feature of HaPyV is its ability to infect both undifferentiated keratinocytes as well as lymphocytes, resulting in the formation of hair follicle and lymphoid tumors. In addition, experimental HaPyV infection in Syrian hamsters has been reported to rarely induce sarcomas and mesothelioma. Mesothelioma is of particular interest in research given the risk of its development in humans following exposure to materials such as asbestos. Interestingly, HaPyV seems to only induce primary mesothelioma in female Syrian hamsters. In addition, transplanted mesotheliomas demonstrate accelerated tumor growth in females. The underlying cause of this sexual predilection is unknown.⁴

In addition to exposure of naïve hamsters to contaminated feces and/or urine, horizontal transmission of HaPyV may also occur due to fighting and/or grooming behavior. As noted by the contributor, subclinical animals, which are often older, may persistently shed the virus into the environment due to harboring it in the renal tubular epithelium. In regard to trichoepitheliomas, the viral infection induces the proliferation of follicular keratinocytes, particularly at the hair root epithelium. Viral particles are most concentrated in the stratum corneum and are absent in the proliferating cells of the stratum

basale. In regard to lymphoma, large and immature neoplastic cells of B- or T-cell origin frequently invade local tissues and metastasis is common. Studies in transgenic mice have found HaPyV demonstrates a tropism for the spleen and thymus, evidenced by the preferential expression of HaPyV extrachromosomal DNA in these locations.⁴

Introduction of HaPyV to a colony can be detrimental, with mortality rates amongst young hamsters due to lymphoma reaching up to 80% within 4-30 weeks of exposure. There are no treatment options for HaPyV infection and culling affected animals is recommended.^{2,4} As noted by the contributor, once the virus becomes endemic the incidence of lymphoma decreases while trichoepithelioma increases, which is likely the result maternal antibody protection. Once enzootic, the virus cannot be controlled without the entire population being culled and the entire premises undergoing thorough decontamination. However, recurrent outbreaks have been reported following these extreme measures, likely due to the resistance of this virus to environmental decontamination.²

Detection of HaPyV virus particles via electron microscopy is a challenge. In addition, evaluation of HaPyV induced lymphoma with the intent of demonstrating viral particles is an ill advised endeavor since lymphoma induction occurs without viral replication. However, viral replication does occur within keratinizing epithelial cells of follicular tumors, often forming characteristic paracrystallin arrays within the nucleus.² In addition to polyomaviruses, other viruses that form characteristic hexagonal paracrystallin arrays include adenovirus, papillomavurs, picornavirus, iridovirus, and circovirus.

Participants identified regions of sebaceous differentiation within the follicular neoplasms and therefore preferred the diagnosis of the trichofolliculoma rather than trichoepithelioma. Trichofolliculoma and trichoepithelioma are both characterized by differentiation to all three segments of the hair follicle, with the former exhibiting pilosebaceous subunits and/or more advanced trichogenesis whereas the latter may exhibit incomplete or abortive trichogenesis and a lack of sebaceous differentiation.

References:

1. Barthold SW, Bhatt PN, Johnson EA. Further evidence for papovavirus as the probable etiology of transmissible lymphoma of Syrian hamsters. *Lab Anim Sci.* 1987;37(3):283-288.
2. Barthold SW, Griffey SM, Percy DH. Pathology of laboratory rodents and rabbits. Fourth edition ed. Ames, Iowa, USA: Wiley Blackwell; 2016.
3. Fox JG, Anderson LC, Otto GM, Pritchett-Corning KR, Whary M, T. Laboratory animal medicine. Third edition ed. Amsterdam ; Boston ; Heidelberg ; London: Elsevier, Academic Press; 2015.
4. Jandrig B, Krause H, Zimmermann W, Vasiliunaite E, Gedvilaite A, Ulrich RG. Hamster Polyomavirus Research: Past, Present, and Future. *Viruses.* 2021;13(5):907.
5. Park C, Li S, Cha E, Schindler C. Immune response in Stat2 knockout mice. *Immunity (Cambridge, Mass.).* 2000;13(6):795-804.
6. Quesenberry K, Carpenter J. Ferrets, rabbits, and rodents. 3rd ed. Elsevier Health Sciences; 2012.
7. Scherneck S, Ulrich R, Feunteun J. The hamster polyomavirus—a brief review of recent knowledge. *Virus Genes.* 2001;22(1):93-101.
8. Simmons JH, Riley LK, Franklin CL, Besch-Williford CL. Hamster polyomavirus infection in a pet syrian hamster (*Mesocricetus auratus*). *Veterinary pathology.* 2001;38(4):441-446.
9. Toth K, Lee SR, Ying B, et al. STAT2 knockout syrian hamsters support enhanced replication and pathogenicity of human adenovirus, revealing an important role of type I interferon response in viral control. *PLoS pathogens.* 2015;11(8).

CASE III: MS19-3845/MS19-3861 (JPC 4136807)

Signalment:

6 week old and 5 month old, male, C57Bl/6 mice

History:

Two mice were infected IP with 1,000 blood trypomastigotes of *Trypanosoma cruzi*. A month later, one mouse was euthanized when it developed clinical signs and the other was found dead.

Gross Pathology:

There was pale tan streaking of the semimembranosus, semitendinosus, and portions of the biceps femoris on both hind legs. The iliopsoas and the hypaxial muscles of the lumbar region also had pale streaking.

No other lesions were present.

Laboratory Results:

None submitted.

Microscopic Description:

Skeletal muscle: There are multifocal – coalescing areas where muscle has undergone one of the following changes: loss of striations, hypereosinophilia, fragmentation, necrosis and mineralization. Within

some muscle fibers, there are large, up to 250um, pseudocysts containing numerous amastigotes. Amastigotes are round, 2-4um with a central nucleus and adjacent kinetoplast. In some areas, the amastigotes appear to be transforming into trypomastigotes. Between the degenerating and necrotic muscle fibers, there are numerous macrophages with fewer lymphocytes, neutrophils, and plasma cells. Regeneration was not seen.

Other lesions:

Heart: myocarditis, moderate with amastigotes

Right atrium: multiple thrombi

Pancreas: acinar loss, moderate

Spleen: plasmacytosis, mild

Contributor's Morphologic Diagnoses:

Skeletal muscle: myositis, multifocal and focally extensive, severe with amastigotes and trypomastigotes.

Contributor's Comment:

Chagas disease or American trypanosomiasis is caused by the flagellate protozoan *Trypanosoma cruzi*. Transmission is by triatomine insects (*Triatoma infestans*, *Rhodnius prolixus*, *Triatoma dimidiata* and *Parastrongylus*), also known as assassin or kissing bugs.⁵ Infection cycles between human, wild, and domestic animal hosts.^{1,2}

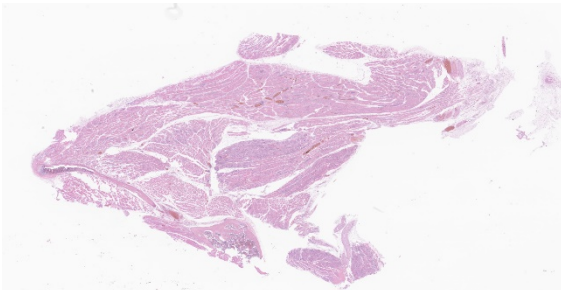


Figure 3-1. Skeletal muscle, mouse. One section of skeletal muscle (with long bone at bottom) is submitted for examination. At low magnification, scattered myofibers are basophilic and hypercellular. (HE, 5X)

The primary route of infection is by bug bite (70%). Less common modes of transmission include congenital (26%) and, accounting for less than 1% of cases, transfusion/organ transplantation, sexual, and laboratory accident.^{4,8} Outbreaks have also been caused by ingestion of contaminated food.^{3,4}

Of those who are infected, 70-80% never develop clinical disease. The other 20-30% progress over years to develop chronic disease in which they commonly develop cardiomyopathy. A small percentage (10%) develop gastrointestinal disease with or without associated cardiomyopathy.^{3,4}

Bugs become infected while taking a blood meal and ingesting blood trypomastigotes. The trypomastigotes mature in the midgut becoming epimastigotes and then, as they pass through the hindgut, develop into infective trypomastigotes. The trypomastigotes are then deposited with feces as the bug takes a second meal. Infection occurs when feces are rubbed into broken skin or mucosa. At the inoculation site, trypomastigotes infect nucleated cells via fusion of host cell lysosomes⁹, transform into amastigotes, divide by binary fission, develop flagella, and then are released as infective trypomastigotes back into the blood to travel to other tissues or infect local cells. Infection by feces (Sterocorarian transmission) is inefficient and is estimated to be between 1-4% per year.³

Chagas disease can be separated into acute, indeterminate, and chronic phases. Acute phase: After being infected, symptoms may not develop but, if they do, they are most often nonspecific.⁵ Rarely, after a 1-2 week incubation period, there may be swelling around the wound the site (Chagoma) or of the eye (Romana's sign).³ Biopsy samples from a Chagoma have intrahistiocytic amastigotes and lymphocytes. Swelling

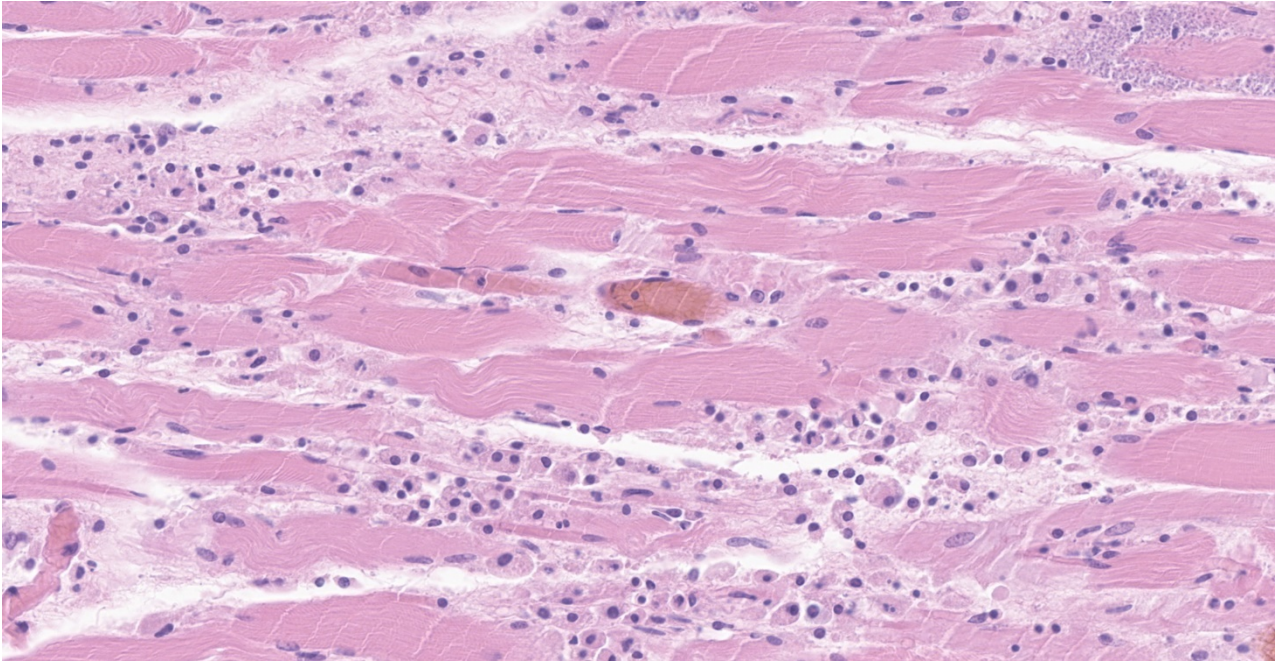


Figure 3-2. Skeletal muscle, mouse. Diffusely, myofibers demonstrate large numbers of macrophages, which occasionally replace myofibers, infiltrates degenerative and atrophic changes and the epimysium. (HE, 280X)

around the eyelid is due to edema and conjunctivitis. A morbilliform rash (schizotrypanides) may also develop. Reported microscopic changes are nonspecific, vascular dilation, edema with perivascular lymphoplasmacytic aggregates. Parasites have been reported not to be associated with the rash.⁸

During the acute phase, approximately 1% of those infected (mostly young infants) develop acute lymphadenopathy, hepatosplenomegaly, encephalitis, myocarditis and heart failure.^{3,4}

The acute phase lasts approximately 4-8 weeks and then disappears presumably due to a cell mediated response.³ Eosinophilia is not reported to be associated with the initial immune response.⁸ During this time, infection can be detected by seeing the organisms in a Giemsa-stained blood or CSF smear and PCR and culture.³

Indeterminant phase: This phase lasts years or for the rest of an individual's lifetime.

Although they are infected, there are no clinical signs. Parasites are not found in blood smears. PCR and serological results are variable. Infection may become reactivated in immunosuppressed individuals who then go on to develop acute disease with fever, erythematous nodules/plaques, myocarditis and encephalitis associated with numerous amastigotes.^{3,4}

Chronic phase: This phase develops after years of being infected. Clinical presentation may include one or more of the following: cardiac conduction abnormalities, dilated cardiomyopathy, left ventricular aneurysm, and congestive heart failure. Thromboembolism and stroke may develop secondarily.^{3,4}

Early myocardial changes include degeneration and necrosis with infiltration primarily of macrophages and neutrophils and, with more chronic lesions, T-cells, eosinophils and plasma cells. Early inflammatory and myocyte changes may be replaced by mild fibrosis, myocyte

hypertrophy and minimal – mild inflammation. More chronic lesions have focally extensive muscle atrophy and loss with thick, transmural fibrosis. Often, in this chronic phase, there may be no inflammation and very few or no parasites. Even by PCR, the organisms are not always detected.⁴ Repeated serologic and PCR tests may be needed to detect chronic infection.³

Gastrointestinal disease may be seen in 10% of those who are infected whether they have cardiac disease or not. Although megacolon and megaesophagus are the most common gastrointestinal presentations, dilation anywhere along the intestinal tract can occur. Infection of the enteric nervous system results in denervation of the intestines and to dilation.^{3,4}

T. cruzi can infect any nucleated cell in the body and, in the heart, it invades the myocytes, nerves, endothelial cells and adipocytes. Why the organism targets myocytes may be due plasma membrane repair mechanisms which allow for entry of the parasite into the cell.⁴

The pathogenesis of *T. cruzi* is incompletely understood but it involves complicated and intertwined mechanisms involving the virulence of the strain of *T. cruzi*, the route of infection and the number of organisms, re-infection, the unique innate and acquired immune responses of the host, and the persistence of the organism within tissues. Initial responses to infection are T-cell mediated which reduce but do not clear infection. Many immune responses of the host (cytokines, chemokines, reactive oxygen molecules and antibodies) do not kill all parasites and end up enhancing the infectivity of and damages caused by it.^{1,3} Adipose tissue has been identified as a reservoir for the parasites.⁴

The World Health Organization has designated Chagas disease as one of the top neglected tropical diseases. Chagas is associated with poverty where housing with cracked walls and thatched roofs allow bugs to live in close proximity to people.¹⁰ Since the institution of insecticide and bed net use along with screening of blood donors and pregnant women, the number of people infected has decreased significantly.³ Still, according to the CDC, 8 million people in Mexico, Central and South America are infected. Migration away from these endemic areas has led to individuals, most of whom are not aware that they are infected, to be identified in North America, Europe, Japan, and Australia. In the United States, 300,000 people are believed to be infected. In addition, triatomine insects can be found in most states and any domestic or wild mammal can be infected and serve as a reservoir/host.^{1,5} In the United States and in other regions where Chagas disease is now found but is not widespread, control strategies are focused on preventing transmission from blood transfusion, organ transplantation, and from mother to baby.⁵ Currently, blood donors are screened for parasites/antibodies. As of 2017, only six states (Arizona, Arkansas, Louisiana, Mississippi, Tennessee and Texas) have designated Chagas as a reportable disease.^{2,3}

Treatment with benznidazole or nifurtimox may lead to 80 – 100% cure in newborns and those known to be acutely infected. Benznidazole may decrease the rate of cardiomyopathy progression.³

Currently, there is no vaccine for Chagas. The inability to predict who will progress from the indeterminate phase and develop cardiac disease continues to be problematic. To date, a definitive molecular marker to

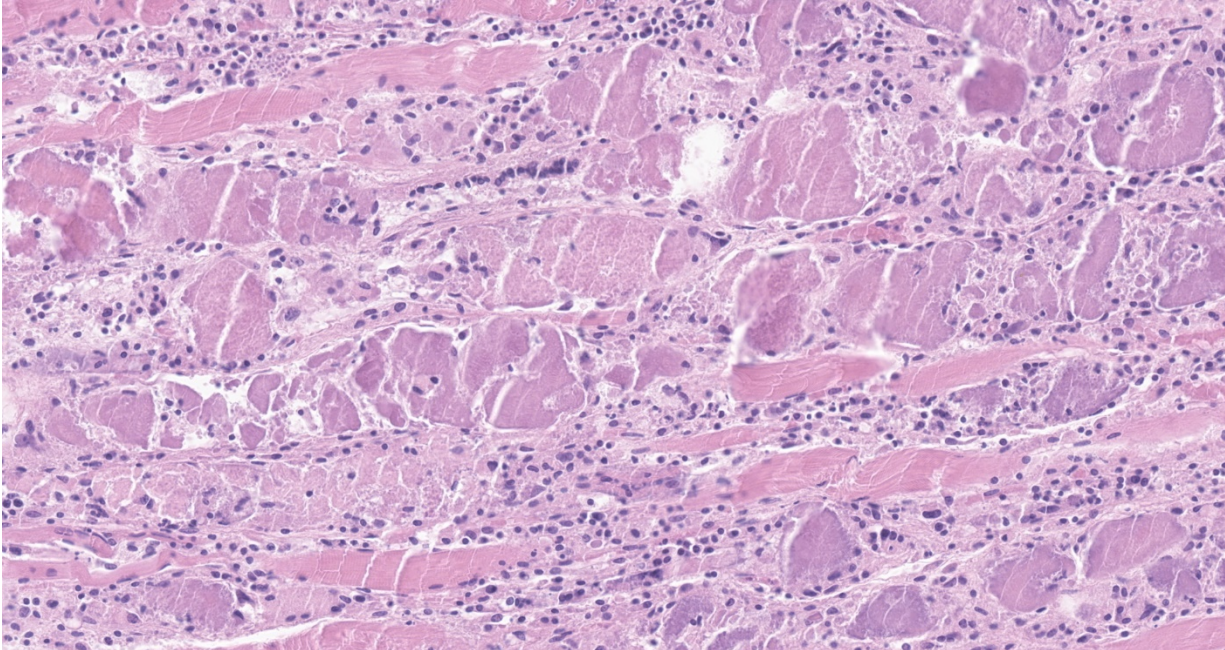


Figure 3-3. Skeletal muscle, mouse. Myocytes are multifocally necrotic and mineralized. The endomysium and numerous myofibers is infiltrated by macrophages. (HE, 226X)

identify those who will or are developing cardiac disease has yet to be identified although, microRNA-2208a, a plasma marker for cardiac disease, has been suggested.⁴

Contributing Institution:

National Institutes of Health
Division of Veterinary Resources
Building 14E/119B
Bethesda, MD 20892
starostm@mail.nih.gov
Phone: 301-443-7251

JPC Diagnosis:

Skeletal muscle: Rhabdomyositis, necrotizing and histocytic, multifocal, moderate, with intrasarcoplasmic and extracellular protozoal amastigotes and myofiber mineralization.

JPC Comment:

The contributor provides an outstanding review of Chagas disease, an emerging disease in the southwestern United States that

historically was restricted to Central and South America.

Chagas disease far predates the arrival of Europeans in the New World, as *T. cruzi* kinetoplast DNA has been identified in exhumed Peruvian and Chilean mummies from approximately 7000 BCE, with similar findings in Central America. It is likely humans became part of the sylvatic cycle of Chagas disease as they began populating the South American coast approximately 9500 years ago. Interestingly, the Andeans domesticated rodents for both consumption and ritualistic use, which likely further attracted hematophagous insects such as *Triatoma infestans*, which are adept at survival in traditional wattle and daub houses.⁶

Interestingly, Charles Darwin may have unknowingly contracted Chagas disease during his famed expedition aboard the HMS *Beagle*. While visiting in the Chilean port city of Valparaiso in 1834, he became severely ill and was bedridden for 7 weeks for

what was thought to be typhoid disease, although no other crew members became ill. In addition, a March 1835 journal entry describes a nocturnal attack of a reduviid bug as “the most disgusting to feel soft wingless insects about one inch long crawling over one’s body; before sucking they are quite thin, but afterwards round and bloated with blood, and in this state they are easily squashed”. Additional exposure likely occurred as he studied *T. infestans*, known at the time as the “great black bug of the Pampas”, for at least four months. Darwin reported no additional symptoms consistent with Chagas disease from 1835-1841, which is consistent with the indeterminate phase as described by the contributor. Between 1841-1861, Darwin experienced symptoms consistent with the chronic phase of Chagas disease, including heart palpitations, extreme fatigue, and vomiting. Given his family’s history of psychiatric tendencies, physicians believed he was suffering from hypochondriasis. However, Darwin’s symptoms persisted and he was later diagnosed with heart failure prior to his death in 1882.

Although it is uncertain if Darwin was truly infected with *T. cruzi*, the history of exposure to a reduviid bug and progression of clinical signs consistent with the acute, indeterminate, and chronic phases of infection are highly consistent.⁶

During the early 1900s, a young Dr. Carlos Chagas was one of several Brazilian physicians dispatched to investigate a malaria outbreak delaying construction of the Brazil Central Railroad in the state of Minas Gerais. During his travels, Dr. Chagas was notified of a nocturnal hematophagous insect found to contain a flagellated parasite similar to one he had previously described in monkeys and named *Trypanosoma minensis*. Samples were sent to his mentor and director of the National Institute of Serum Therapy in Rio, Dr. Osvaldo Cruz, who then inoculated several laboratory monkeys. A month later, Dr. Chagas found the parasite within the blood of the monkeys was different than *T. minensis*, and named the parasite *T. cruzi* to honor his mentor. Dr. Chagas proceeded to seek a human host and later found the parasite

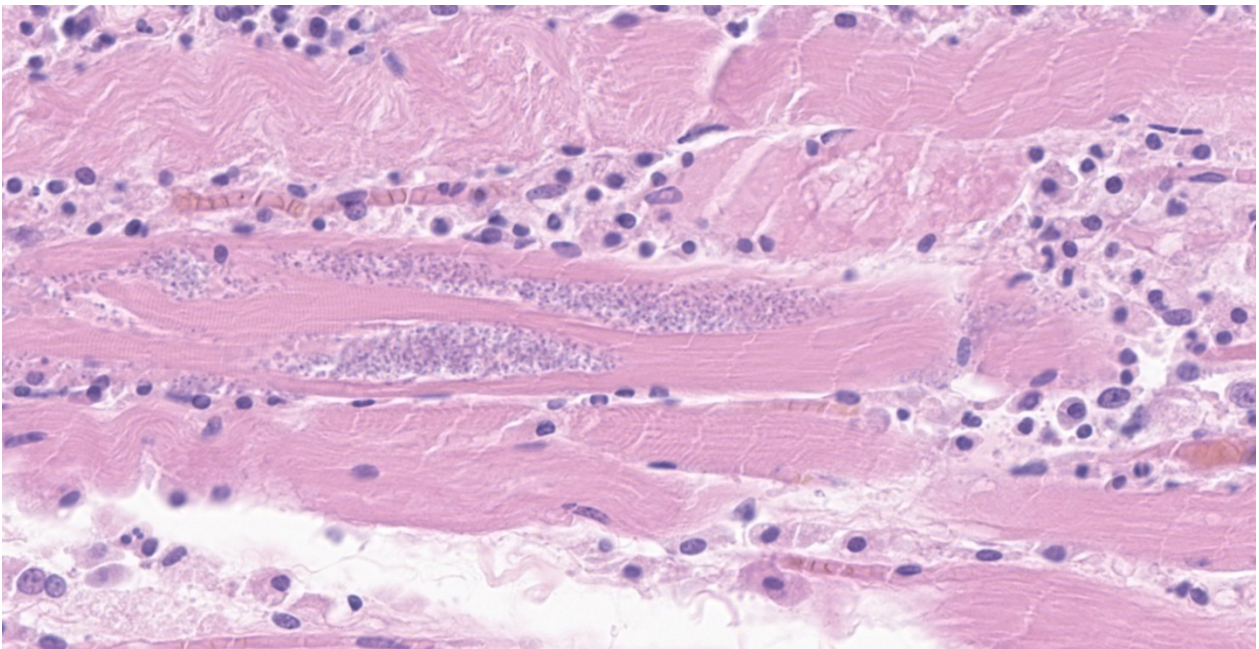


Figure 3-4. Skeletal muscle, mouse. Scattered myocytes contain numerous intracytoplasmic amastigotes consistent with *T. cruzi*. (HE, 400X)

in the blood of a two-year-old girl named Berenice, who had fever, facial edema, and hepatic-splenic-lymph node syndrome. Dr. Chagas is therefore credited with performing a “reverse triple discovery” by first identifying the vector, followed by the parasite, and finally the host.⁶

As noted by the contributor, iatrogenic transmission of Chagas disease has been of growing concern, with reports of *T. cruzi* transmission via kidney transplants in Brazil during the 1980s, with similar reports of accidental transmission occurring in the United States 20 years later. In addition, large numbers of individuals in endemic areas on organ transplant waitlists are infected, including 7% of Argentinians. This is a concern, given the risk of reactivation occurring as the result of transplant related immunosuppression, which is reported to occur in 23-75% of patients. However, treatment with benznidazole for 30-60 days is effective, with only 0.3% mortality associated with Chagas disease reactivation.⁶

References:

1. Acevedo GR, Girard MC, Gómez KA. The Unsolved Jigsaw Puzzle of the Immune Response in Chagas Disease. *Front Immunol*. 2018;9:1929.
2. Bennett C, Straily A, Haselow D, et al. Chagas Disease Surveillance Activities - Seven States, 2017. *MMWR Morb Mortal Wkly Rep*. 2018;67(26):738-741.
3. Bern C. Chagas' Disease. *N Engl J Med*. 2015;373(19):1882.
4. Bonney KM, Luthringer DJ, Kim SA, Garg NJ, Engman DM. Pathology and Pathogenesis of Chagas Heart Disease. *Annu Rev Pathol*. 2019;14:421-447.
5. CDC. American Trypanosomiasis. <https://www.cdc.gov/dpdx/trypanosomiasisamerican/index.html>

6. Chao C, Leone JL, Vigliano CA. Chagas disease: Historic perspective. *Biochim Biophys Acta Mol Basis Dis*. 2020;1866(5):165689.
7. Gomes C, Almeida AB, Rosa AC, Araujo PF, Teixeira ARL. American trypanosomiasis and Chagas disease: Sexual transmission. *Int J Infect Dis*. 2019;81:81-84
8. Hemmige V, Tanowitz H, Sethi A. Trypanosoma cruzi infection: a review with emphasis on cutaneous manifestations. *Int J Dermatol*. 2012;51(5):501-508.
9. Rassi A Jr, Rassi A, Marin-Neto JA. Chagas disease. *Lancet*. 2010;375(9723):1388-1402.
10. World Health Organization https://www.who.int/neglected_diseases/2010report/en/

CASE IV: WSC2017-18 Case 2 (JPC 4100655)

Signalment:

Adult female cynomolgus macaque (*Macaca fascicularis*).

History:

This animal was the positive control animal in an Ebola-Zaire vaccine study. All animals in the study were determined to be immunocompetent, confirmed by polyclonal lymphocyte activation *in vitro*, and seronegative for all retroviruses. The animal was inoculated intramuscularly with Ebola-Zaire and was euthanized six days later.

Research was performed under an Institutional Animal Care and Use Committee approved protocol in compliance with the Animal Welfare Act and other federal statutes and regulations relating to animals and experiments involving animals and adheres to principles stated in The Guide for the Care and Use of Laboratory Animals,

National Research Council, 1996. The facility where the research was conducted is fully accredited by the Association for Assessment and Accreditation of Laboratory Animal Care, International.

Gross Pathology:

Upon gross examination, the following findings were recorded: mild reddening of the skin of the inner arms, face, and abdomen, diffusely tan and friable liver, mildly enlarged spleen, petechial hemorrhages of the urinary bladder mucosa, multifocal bilateral tan discoloration of kidneys, multiple reddened enlarged lymph nodes, and subcutaneous and intramuscular hemorrhage in the area of inoculation.

Laboratory Results:

None submitted.

Microscopic Description:

Liver with gallbladder: There are multifocal to coalescing, random areas of necrosis affecting approximately 25% of this section consisting of hepatocytes that are either individualized, shrunken, and hyper-eosinophilic (necrotic) or swollen with vacuolated cytoplasm (degenerate); and admixed with eosinophilic cellular and karyorrhectic debris, fibrin, and few neutrophils, lymphocytes and macrophages. Many hepatocytes, especially those within or adjacent to areas of necrosis, contain single or multiple variably sized, up to 7 um diameter, eosinophilic round to oval intracytoplasmic viral inclusion bodies. Diffusely, hepatic sinusoids are mildly expanded by fibrin and neutrophils. The majority of remaining hepatocytes contain a single or multiple discrete, clear lipid vacuoles which infrequently compress and peripheralize the nucleus. Multifocally, few arteries and veins contain fibrin, have a loss of integrity of the endothelial lining, and their walls are transmurally infiltrated by neutrophils, lymphocytes, macrophages,

necrotic cellular debris, fibrin, and hemorrhage (necrotizing vasculitis).

Contributor's Morphologic Diagnoses:

Liver: Hepatitis, necrotizing, multifocal to coalescing, moderate, with acute hepatitis, vasculitis, and hepatocyte intracytoplasmic viral inclusions.

Contributor's Comment:

The presented case demonstrates the typical hepatic necrotizing lesion of acute Ebolavirus (EBOV) infection in the *Cynomolgus* macaque. Inflammation is often absent to minimal. Cytoplasmic viral inclusions are most prominently identified within hepatocytes, although their presence in macrophages, to include within other infected organs, has been documented. Viral antigen is observed in many cell types in this case, to include hepatocytes, Kupfer cells, sinusoidal lining cells and endothelial cells. In comparison to the negative control for EBOLA antigen, there is strong positive immunoreactivity also within the serum diffusely within the sinusoids and blood vessels.

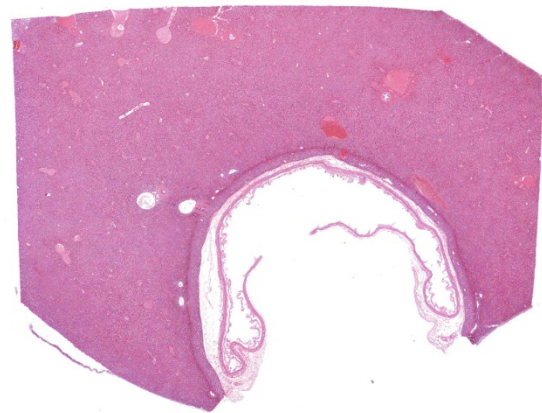


Figure 4-1. Liver and gallbladder, cynomolgus macaque. A section of liver and gallbladder is submitted for examination – there are no lesions visible at this magnification, but there is marked acute congestion of the liver. (HE, 5X)

With regard to infectious diseases, few share the abilities of EBOV to cause global disruption, blanket international headlines, and strike fear into the world population as it does during epidemics. There have been 25 such epidemics since its discovery during simultaneous outbreaks in Zaire, Africa (now the Democratic Republic of the Congo) and Sudan in 1976.² All have occurred along the equatorial belt of Africa, but the 2013 West Africa epidemic eclipsed them all as the most geographically extensive, fatal, and longest lasting in Ebola's history²; injecting a greater sense of urgency into the international community to identify therapeutics and vaccines.

EBOV is a filovirus (single-stranded, negative-sense RNA virus), but is also a member of the viral group known to cause viral hemorrhagic fever.^{2,9} That group includes Dengue, Lassa, and Yellow Fever among others; and while all emerge from different reservoirs with variable pathogenesis, they all feature severe systemic viral infection associated with hemorrhagic

phenomena such as petechiae, ecchymoses and frank bleeding.² There are 5 species of EBOV: Bundibugyo, Reston, Sudan, Tai Forest and Zaire.⁹ All but Reston are pathogenic to humans.¹ Zaire EBOV is the most common cause of epidemics and also the culprit of the most recent one in West Africa.²

Both Rhesus and *Cynomolgus* macaques are considered the gold standard model of EBOV disease for their consistent similarity to human disease.² Nonhuman primates (NHP) may play a role in the natural history of EBOV, but no mammalian reservoir has yet been identified and most recent studies implicate fruit bats.^{6,7} Following an unknown route of exposure from a reservoir species to a human or NHP, viral transmission between these species occurs via inoculation into the bloodstream or exposure to mucus membranes or nonintact skin.² Aerosol transmission has been described experimentally but never recorded in humans and only described in one study in NHP's.⁹ NHP's develop fever, diarrhea and macular

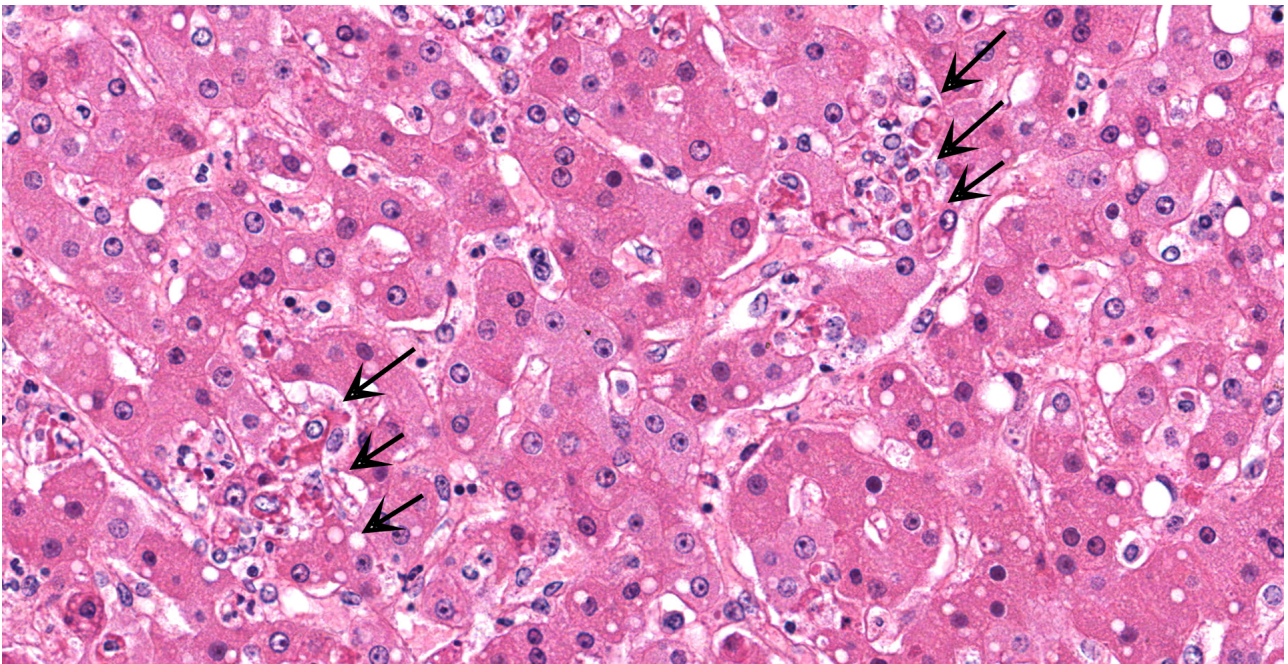


Figure 4-2. Liver, cynomolgus macaque. There are multifocal randomly scattered foci of lytic necrosis of hepatocytes (arrows). (HE, 405X)

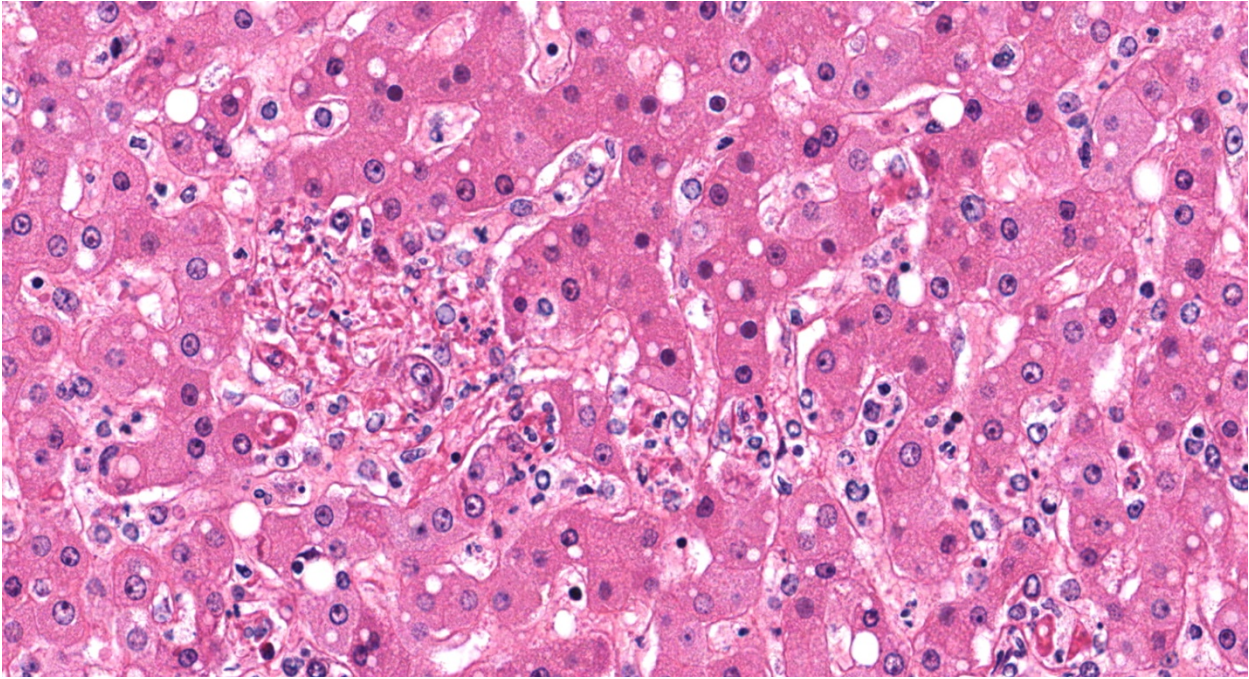


Figure 4-3. Liver, cynomolgus macaque. Another, larger focus of hepatic lytic necrosis with fibrin streaming into sinusoids. Increased numbers of neutrophils circulate within sinusoids and Kupffer cells are hyperplastic.

rash along with leukocytosis, lymphopenia, thrombocytopenia and elevated D-Dimers typically within 6 days post-inoculation.³ Fatality rates are greater than 90% in *Macaca* spp., and death invariably occurs between 7-10 days post infection.³

The hallmark lesions of EBOV in NHP's include petechial and/or ecchymotic hemorrhages of the mucous membranes, internal organs, and skin; widespread lymphocytolysis in the lymph nodes and spleen; splenic fibrin deposition of the red pulp; hepatic necrosis; hepatocytic viral inclusions; and hemorrhage and congestion of the submucosa throughout the gastrointestinal tract, most prominently in the duodenum.³ Ocular lesions of necrotizing scleritis and conjunctivitis have been described in recovering Rhesus Macaques which parallels similar late onset lesions in humans.^{1,2}

EBOV initially targets dendritic cells and macrophages which then disseminate to lymphoid tissues where viral replication

occurs. The virus quickly becomes widely disseminated in the bloodstream; and multiple organs, especially the liver and spleen, are targeted as multiple cell types within these organs to include endothelial cells become infected. Lymphocytes are the rare cell type that avoids viral infection.²

The major mediators of EBOV tissue damage and disease manifestation include proinflammatory cytokines (TNF- α , IL-1, IL-6 & MCP/MIP), nitric oxide, tissue factor, increased TRAIL or Fas-FasL expression, and the EBOV glycoprotein.² Tissue damage is further enhanced by ischemia; a culminating effort from tissue factor activation, fibrin thrombus formation, hepatic necrosis, and consumption of platelets and clotting factors. Late-appearing hemorrhages are thought to represent disseminated intravascular coagulation.²

EBOV induces a robust immune response capable of clearing infection in all but immunologically privileged organs (eye, testis, etc.). When the infection is identified early and supportive medical care is available, survival can be expected for many if not most patients. The case-fatality ratio among those 27 patients treated in Europe or the United States during the last epidemic was just 18.5%, stark contrast to the 40% range among those patients remaining in West Africa or the more historical 88% fatality rate for the earliest outbreaks.² Targeted therapies may have contributed to this success; replication inhibitors, plasma infusion, and a recent cocktail of three monoclonal antibodies known as ZMapp have all been shown experimentally to reduce mortality in mice and/or NHP's.² Documented success attributed to these has

been less fruitful among humans thus far, however.

While no vaccine has yet been licensed, there are currently 11 different EBOV vaccines undergoing clinical study. Four are in phase III testing, and one focusing on the EBOV glycoprotein has gained widespread recognition due to documentation of 100% efficacy in a ring vaccination trial during the recent West Africa epidemic.⁴ Much of the natural history and pathogenesis of EBOV remains an enigma, however. Even if an effective vaccine becomes commercially available, the economic and logistical challenges of the endemic regions will likely continue to necessitate their rapid deployment following an epidemic emergence until more is understood regarding the underlying causes which may contribute to their prevention altogether.

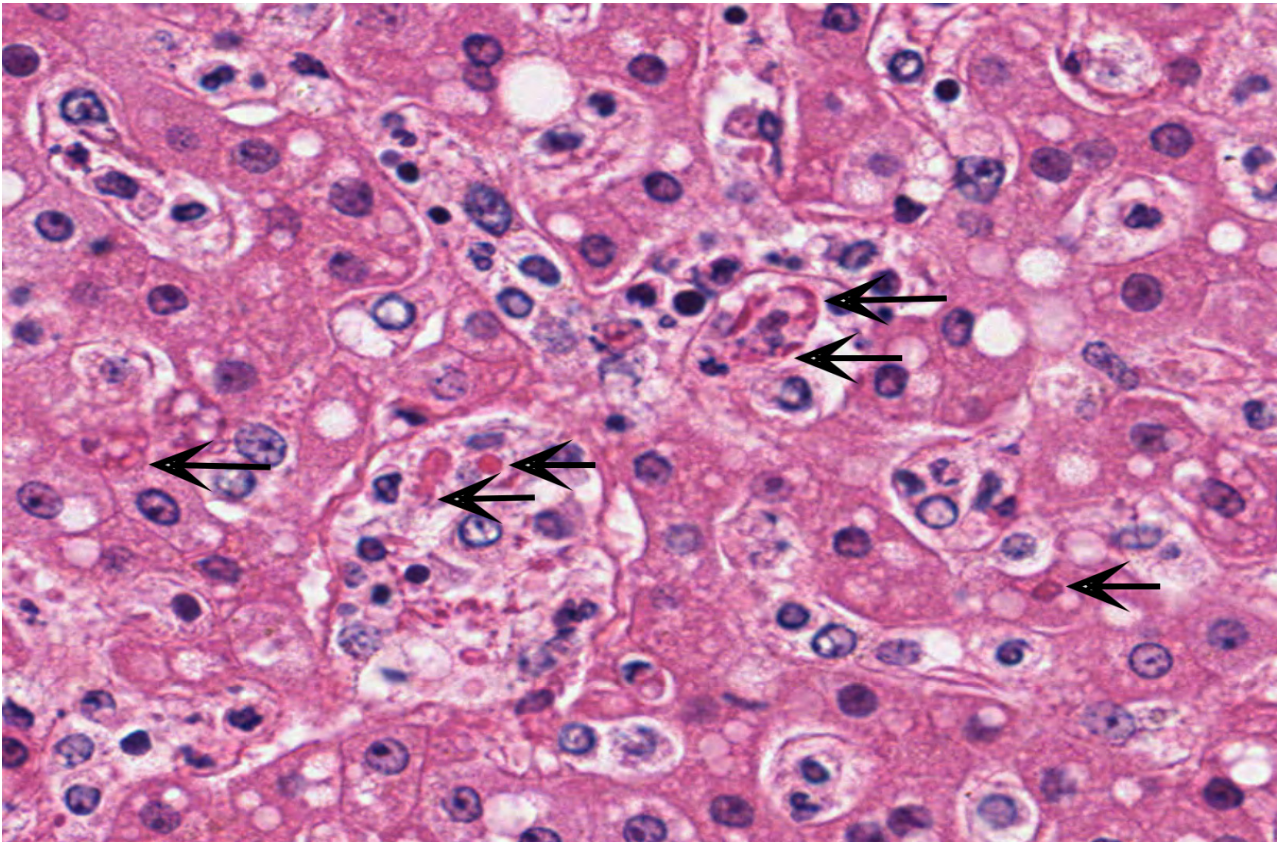


Figure 4-4. Liver, cynomolgus macaque. Degenerating hepatocytes contain one to multiple 2-6µm intracytoplasmic viral inclusions. (HE, 500X)

Contributing Institution:

US Army Medical Research Institute of Infectious Diseases (USAMRIID)

Fort Detrick, MD

<https://riid-vision.detrick.army.mil/pathology>

JPC Diagnosis:

Liver: Hepatitis, necrotizing, random, multifocal, severe, with vasculitis and numerous intracytoplasmic viral inclusions.

JPC Comment:

The contributor provides a thorough and outstanding review of *Ebolavirus* (EBOV), the second filovirus reviewed by the Wednesday Slide Conference in three weeks (see 21-22 WSC Conf. 17-1 *Marburgvirus*).

Since the submission of this case in 2017, two vaccines for *Zaire* EBOV have been licensed: Ervebo and the two dose vaccine regimen of Zabdeno and Mvabea.¹⁰

Ervebo is a single dose vaccine that utilizes an attenuated-live recombinant stomatitis virus-based vector that expresses the envelope glycoprotein (GP) gene of *Zaire* EBOV.⁷ Consequentially, Ervebo has not been demonstrated to provide protection against disease caused by filoviruses other than *Zaire* EBOV.⁹ Regarding the 2-dose vaccine regimen, Zabdeno is monovalent replication incompetent adenoviral vector vaccine that encodes the full length GP of the Mayinga variant of *Zaire* EBOV. The second dose, Mvabea, is a multivalent *Modified Vaccinia Ankara* virus vaccine that similarly encodes for the GP of the Mayinga variant of *Zaire* EBOV, in addition to the Gulu GP of *Sudan* EBOV, Musoke GP of *Marburgvirus*, and the nucleoprotein of *Tai Forest* EBOV.⁸

Ervebo was first utilized under a “compassionate use” protocol for 16,000 people in Guinea during a 2015 EBOV outbreak, with similar utilization during the 2018-2020 outbreak in the Democratic Republic of Congo with the immunization of 345,000 individuals. Ervebo was licensed in November 2019 by the European Medicines Agency, followed shortly thereafter by the United States Food and Drug Administration, as well as in multiple West African nations. Due to limited quantities of available vaccine, Ervebo is not utilized in a traditional manner with mass vaccination campaigns. Instead, the vaccine is maintained as part of a strategic stockpile reserved for outbreak response focused on establishing a “ring vaccination” strategy, similar to the approach used to eradicate smallpox. Notably, “ring vaccination” does not imply vaccination of individuals within a specific geographic area following identification of a positive case. Instead, extensive contact tracing is used to identify individuals with a high risk of exposure, such as those in close contact with an infected person’s body, body fluids, linen, or clothes over a 21 day period. Historically, each positive case is typically associated with approximately 150 individuals deemed to be at high risk of exposure.¹⁰

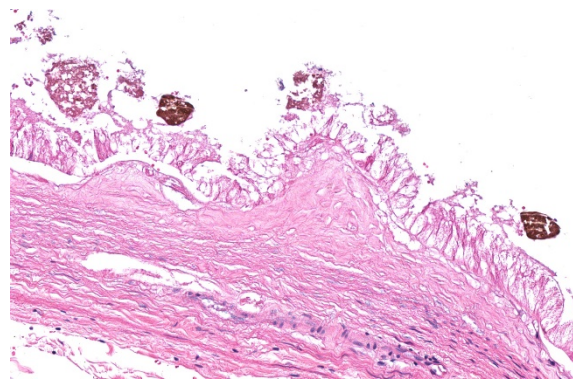


Figure 4-5. Gallbladder, cynomolgus macaque. There are two small choleliths adjacent to the gallbladder mucosa. (HE, 400X)

In May 2020, the European Medicines Agency recommended market authorization for the two dose vaccine regimen of Zabdeno and Mvabea for persons >1 year of age. The first vaccine in the protocol, Zabdeno, is followed approximately 8 weeks later by the second vaccine, Mvabea. Given the prolonged amount of time between the initial vaccination and immunity, the Zabdeno Mvabea 2-dose vaccine regimen is less suitable for outbreak responses than Ervebo. In addition, a booster vaccination of Zabdeno is recommended for individuals at imminent risk of exposure to EBOV (e.g. healthcare workers and those living or visiting areas with an ongoing outbreak) if more than four months have passed since administration of the second dose.¹⁰

Although vaccines are powerful tools for curbing future EBOV outbreaks, they are only one of many components of an effective control strategy. Additional components include early detection of new EBOV infections, functional laboratories to confirm infections, isolation and provision of supportive care for patients, and safely (albeit respectfully) burying the dead in a timely manner to reduce further spread through contact with deceased patients.⁹

As discussed in WSC#17, EBOV and *Marburgvirus* are both reported to persist in immune-privileged tissues of survivors, including the aqueous humor, central nervous system, and testicles. Sexually transmission of both viruses has been reported. In one case, Ebola virus RNA was detected by reverse transcription PCR in semen 531 days following onset of symptoms.³ The moderator used this fairly recent discovery as an example to underscore the importance of collecting samples from as many tissues as possible when operating in a research setting, even those deemed inconsequential at the time of collection. If subsequent discoveries

warrant further investigation, the availability of these tissues for retrospective analysis may not only provide more timely information, but also facilitate subsequent study design and/or reduce the need for additional resources, such as animal models. This practice is of particular importance in studies utilizing NHPs given their limited availability.

References:

1. Alves DA, Honko AN, Kortepeter MG, et al. Necrotizing scleritis, conjunctivitis, and other pathologic findings in Ebola virus-infected rhesus macaque (*Macaca mulatta*) with apparent recovery and a delayed time of death. *J Infect Dis.* 2016;213(1):57-60.
2. Baseler L, Chertow DS, Johnson KM, Feldmann H, and Morens D. The pathogenesis of ebola virus disease. *Annu Rev Pathol Mech.* 2017;12:387-418.
3. Den Boon S, Marston BJ, Nyenswah TG, Jambai A, Barry M, Keita S, et al. Ebola Virus Infection Associated with Transmission from Survivors. *Emerg Infect Dis.* 2019 Feb;25(2):249-255
4. Geisbert TW, Hensley LE, Larsen T, et al. Pathogenesis of Ebola hemorrhagic fever in cynomolgus macaques. *Am J Pathol.* 2003;163(6):2347-2370.
5. Henao-Restrepo AM, Longini IM, Egger M, et al. Efficacy and effectiveness of an rVSV- vectored vaccine expressing Ebola surface glycoprotein: interim results from the Guinea ring vaccination cluster-randomised trial. *Lancet.* 2015;386:857-866.
6. Leendertz SJ, Gogarten JF, Dux A, Calvignac-Spencer S, Leendertz FH. Assessing the evidence supporting fruit bats as the primary reservoirs for Ebola viruses. *Ecohealth.* 2015;13:18-25.
7. Olival KJ, Hayman DT. Filoviruses in bats: current knowledge and future directions. *Viruses.* 2014;6:1759-1788.

8. Tomori O, Kolawole MO. Ebola virus disease: current vaccine solutions. *Curr Opin Immunol.* 2021;71:27-33.
9. Twenhafel NA, Mattix ME, Johnson JC, et al. Pathology of experimental aerosol Zaire Ebolavirus infection in rhesus macaques. *Vet Pathol.* 2012;50(3):514-529.
10. World Health Organization. Ebola virus disease: Vaccines. World Health Organization. Retrieved February 14, 2022, from <https://www.who.int/news-room/questions-and-answers/item/ebola-vaccines>.